

PHENOMENOLOGICAL MODELING OF SHAPE MEMORY ALLOY HELICAL SPRING

Pedro Manuel C.L. Pacheco, *calas@cefet-rj.br*

Department of Mechanical Engineering - CEFET/RJ
20.271.110 – Rio de Janeiro – RJ – Brazil

Marcelo A. Savi, *savi@mecanica.ufrj.br*

Universidade Federal do Rio de Janeiro
COPPE – Department of Mechanical Engineering
21.941.972 – Rio de Janeiro – RJ, Brazil, P.O. Box 68.503

Alberto Paiva, *paiva@lavi.coppe.ufrj.br*

Escola de Engenharia Industrial Metalúrgica de Volta Redonda - UFF
27.255.250 – Volta Redonda – RJ – Brazil

Abstract. *Shape memory alloys (SMAs) are a family of metals with the ability of changing shape depending on their temperature. SMAs undergo thermoelastic phase transformations, which may be induced either by temperature or stress. Because of such remarkable property, SMAs have found a number of applications in different areas. The present contribution focuses on the modeling and simulation of SMA helical springs. Basically, it is assumed a one-dimensional constitutive model to describe its thermomechanical shear behavior and, afterwards, helical springs are modeled considering classical approach. A numerical method based on the operator split technique is developed and numerical results show that the constitutive model is in close agreement with experimental shear tests. Numerical simulations considering a SMA helical springs show that the proposed model captures the general thermomechanical behavior of SMA helical springs. Rate-dependent aspects of the SMA behavior are investigated considering different loading rates.*

Keywords: *Shape memory alloys, smart materials, actuators, constitutive modeling, helical springs*

1. INTRODUCTION

Shape memory alloys (SMAs) present complex thermomechanical behaviors related to different physical processes. Besides the most common phenomena presented by this class of material, such as pseudoelasticity, shape memory effect, which may be one-way (SME) or two-way (TWSME), and phase transformation due to temperature variation, there are more complicated phenomena that have significant influence over its overall thermomechanical behavior – for instance: plastic behavior, tension-compression asymmetry, plastic-phase transformation coupling, transformation induced plasticity, thermomechanical coupling, among others.

The thermomechanical behavior of SMAs has been described by different mathematical models that capture the main behaviors of these alloys. SMA thermomechanical behavior can be modeled either by microscopic or by macroscopic points of view. The first approach, actually, considers either microscopic or mesoscopic phenomena. The microscopic approach treats phenomena in molecular level while mesoscopic approach is related to the level of lattice particles, and its modeling assumes negligible fluctuations of the molecular particles. On the other hand, the macroscopic approach is interested on SMAs' phenomenological features (Paiva & Savi, 2006).

The remarkable properties of SMAs are attracting much technological interest, motivating different applications in several fields of sciences and engineering. Aerospace, biomedical, and robotics are some areas where SMAs have been applied (van Humbeeck, 1999; Machado & Savi, 2002, 2003; Denoyer *et al.*, 2000; Pacheco & Savi, 1997; Garner *et al.*, 2001; Webb *et al.*, 1999; Rogers, 1995).

SMA helical springs are used as actuator devices and its modeling is quite complex. There are some efforts to model the SMA helical spring thermomechanical behavior (Toi *et al.*, 2004, Savi & Braga, 1993a,b; Tobushi & Tanaka, 1991). In the present contribution, it is proposed a simplified model that may be useful for engineering purposes. Basically, a constitutive model originally proposed for one-dimensional tensile-compressive behavior (Savi *et al.*, 2002, Baêta-Neves *et al.*, 2004, Paiva *et al.*, 2005, Savi & Paiva, 2005) is employed to describe shear behavior. Afterwards, it is developed a SMA helical spring model assuming that the spring wire presents a homogeneous phase transformation. Numerical simulations are performed showing that the constitutive model is in close agreement with experimental tests. Moreover, the SMA helical spring model captures the general behavior of this kind of device. Rate-dependent aspects of the SMA behavior are investigated considering different loading rates.

2. CONSTITUTIVE MODEL

There are different ways to describe the thermomechanical behavior of SMAs (Paiva & Savi, 2006). Here, a constitutive model that is built upon the Fremond's model (Fremond, 1987, 1996) and previously presented in different references (Savi *et al.*, 2002, Baêta-Neves *et al.*, 2004, Paiva *et al.*, 2005, Savi & Paiva, 2005) is employed. This model considers different material properties and four macroscopic phases for the description of the SMA behavior. The model also considers plastic strains and plastic-phase transformation coupling, which turns possible the two-way shape memory effect description. Moreover, the original model also contemplates tension-compression asymmetry.

Besides strain (ε) and temperature (T), the model considers four more state variables associated with the volumetric fraction of each phase: β_1 is associated with positive detwinned martensite, β_2 is related to negative detwinned martensite, β_3 represents austenite and β_4 corresponds to twinned martensite. Actually, the original model also includes other variables related to plastic phenomenon, which are beyond the scope of this contribution.

Although this one-dimensional constitutive model is originally proposed to describe tensile-compressive behavior, it has been noted that experimental torsion test curves presented in different references (Jackson *et al.*, 1972; Manach & Favier, 1997) indicate that these curves are qualitatively similar to those obtained in tension tests performed in Ni-Ti and other SMA. Based on this observation, this constitutive model is employed to describe the pure shear stress states, replacing the stress, strain, and elastic modulus respectively by the shear stress τ , shear strain χ and shear modulus G .

In order to obtain the constitutive equations, the same procedure is employed. A free energy potential is proposed concerning each isolated phase. After this definition, a free energy of the mixture can be written weighting each energy function with its volumetric fraction. With this assumption, it is possible to obtain a complete set of constitutive equations that describes the thermomechanical behavior of SMAs as presented below:

$$\tau = G\gamma + (\alpha + G\alpha_h)(\beta_2 - \beta_1) \quad (1)$$

$$\dot{\beta}_1 = \frac{1}{\eta_1} \left\{ \alpha\gamma + A_1 + (2\alpha_h\alpha + G\alpha^2)(\beta_2 - \beta_1) + \alpha_h G\gamma - \partial_1 J_\pi \right\} + \partial_1 J_\chi \quad (2)$$

$$\dot{\beta}_2 = \frac{1}{\eta_2} \left\{ -\alpha\gamma + A_2 - (2\alpha_h\alpha + G\alpha^2)(\beta_2 - \beta_1) - \alpha_h G\gamma - \partial_2 J_\pi \right\} + \partial_2 J_\chi \quad (3)$$

$$\dot{\beta}_3 = \frac{1}{\eta_3} \left\{ -\frac{1}{2}(G_A - G_M)[\gamma + \alpha_h(\beta_2 - \beta_1)]^2 + A_3 - \partial_3 J_\pi \right\} + \partial_3 J_\chi \quad (4)$$

where $G = G_M + \beta_3(G_A - G_M)$ is the shear modulus. Notice that subscript "A" refers to austenitic phase, while "M" refers to martensite. Parameters α and α_h are respectively associated with the vertical and horizontal sizes of the hysteresis loop.

The terms $\partial_n J_\pi$ ($n = 1,2,3$) are sub-differentials of the indicator function J_π with respect to β_n (Rockafellar, 1970). The indicator function $J_\pi(\beta_1, \beta_2, \beta_3)$ is related to a convex set π , which provides the internal constraints related to the phases' coexistence. Concerning the evolution equations of volumetric fractions, η_1 , η_2 and η_3 represent the internal dissipation related to phase transformations. Moreover, $\partial_n J_\chi$ ($n = 1,2,3$) are sub-differentials of the indicator function J_χ with respect to β_n (Rockafellar, 1970). This indicator function is associated with the convex set χ , which establishes conditions for the correct description of internal sub-loops due to incomplete phase transformations and also avoids phase transformations $M^+ \rightarrow M$ or $M^- \rightarrow M$ (Savi & Paiva, 2005).

Concerning the parameters definition, linear temperature dependent relations are adopted for A_1 , A_2 and A_3 as follows:

$$A_1 = A_2 = -L_0^M + \frac{L^M}{T_M}(T - T_M) \quad A_3 = -L_0^A + \frac{L^A}{T_M}(T - T_M) \quad (5)$$

where T_M is the temperature below which the martensitic phase becomes stable, L_0^M , L^M , L_0^A and L^A are parameters related to critical stress for phase transformation.

In order to contemplate different characteristics of the kinetics of phase transformation for loading and unloading processes, it is possible to consider different values to the parameters η_n ($n = 1,2,3$), which are related to internal dissipation: η_n^L and η_n^U during loading and unloading process, respectively. For more details about the constitutive model, see Paiva *et al.* (2005).

3. SHAPE MEMORY ALLOY HELICAL SPRING

The modeling of the restoring force produced by a shape memory alloy spring is done considering a helical spring with diameter D , built with N coils with a wire diameter d . It is assumed that the longitudinal force, F , is resisted by the torsional shear stress developed on the circular cross section of the helical shaped wire (Figure 1) (Shigley, 1972).

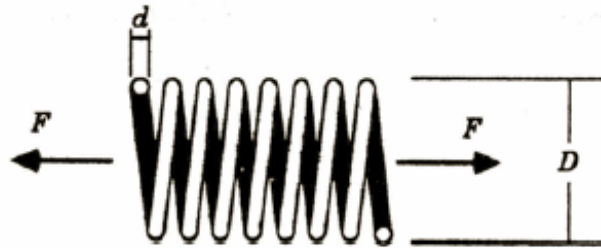


Figure 1. Helical spring.

$$F = \frac{4\pi}{D} \int_0^{d/2} \tau r^2 dr \quad (6)$$

where r is the radial coordinate along the wire cross section. It is also assumed that the shear strain is linearly distributed along the wire cross section, from what follows the kinematics relation

$$\gamma = \frac{d}{\pi D^2 N} u \quad (7)$$

where u is the spring displacement.

By combining these equations, and performing the integration assuming that the wire presents a homogeneous phase transformation through the wire cross section, we obtain:

$$F(u, T, \beta_i) = \frac{\pi d^3}{6D} \left[\left(\frac{d}{\pi D^2 N} G \right) u + (\alpha + G\alpha_h)(\beta_2 - \beta_1) \right] \quad (8)$$

This equation expresses the force-displacement relation for SMA helical springs.

4. NUMERICAL SIMULATIONS

The operator split technique (Ortiz *et al.*, 1983) associated with an iterative numerical procedure is developed in order to deal with the nonlinearities of the formulation. The procedure isolates the sub-differentials and uses the implicit Euler method combined with an orthogonal projection algorithm (Savi *et al.*, 2002) to evaluate evolution equations. Orthogonal projections assure that volumetric fractions of the martensitic variants obey the imposed constraints. In order to satisfy constraints, values of volumetric fractions must stay inside or on the boundary the tetrahedron shown in Figure 2 that establishes the phase coexistence conditions.

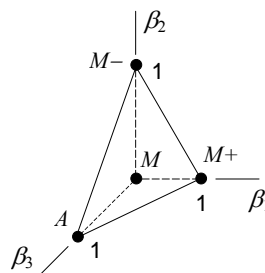


Figure 2. Tetrahedron of the constraints related to phase coexistence.

In order to evaluate the model capability to describe SMA shear behavior, it is performed numerical simulations that are compared with results obtained from experimental tests presented in Manach & Favier (1997). The experimental study of NiTi behavior in simple shear tests are performed at several temperatures using a hydraulic tension-compression machine. Parameters experimentally adjusted for these experimental tests are presented in Table 1, considering quasi-static tests developed by using a triangular loading wave with a 8s period.

Table 1. SMA parameters.

G_A (GPa)	G_M (GPa)	α (MPa)	γ_R	T_M (K)
16	9	30	0.044	292
L_0^M (MPa)	L^M (MPa)	L_0^A (MPa)	L^A (MPa)	
0.7	9.5	0.03	27	
$\eta_{1,2}^L$ (KPa.s)	$\eta_{1,2}^U$ (KPa.s)	η_3^L (KPa.s)	η_3^U (KPa.s)	
3.5	52	3	2	

Quasi-static stress-strain shear curves obtained with the adjusted parameters for three different temperatures are presented in Figure 3: $T = 263\text{K}$, a temperature where martensite is stable for a stress-free state, $T = 333\text{K}$ and $T = 348\text{K}$, temperatures where austenite is stable for a stress-free state. It is noticeable the close agreement between numerical and experimental results. Discrepancies are probably due to some phenomena not included in the present formulation such as transformation induced plasticity and thermomechanical coupling.

After the stress-strain analysis, the proposed formulation for the spring is employed to analyze the spring response. It is considered a helical spring with a diameter, $D = 8$ mm, a wire diameter, $d = 1$ mm, an unstretched length, $L = 28$ mm and $N = 16$ coils. Figure 4 shows the force-displacement curves for the three temperatures (263 K, 333 K and 348 K). As expected, the force-displacement curves have the same qualitative behavior of the stress-strain curves.

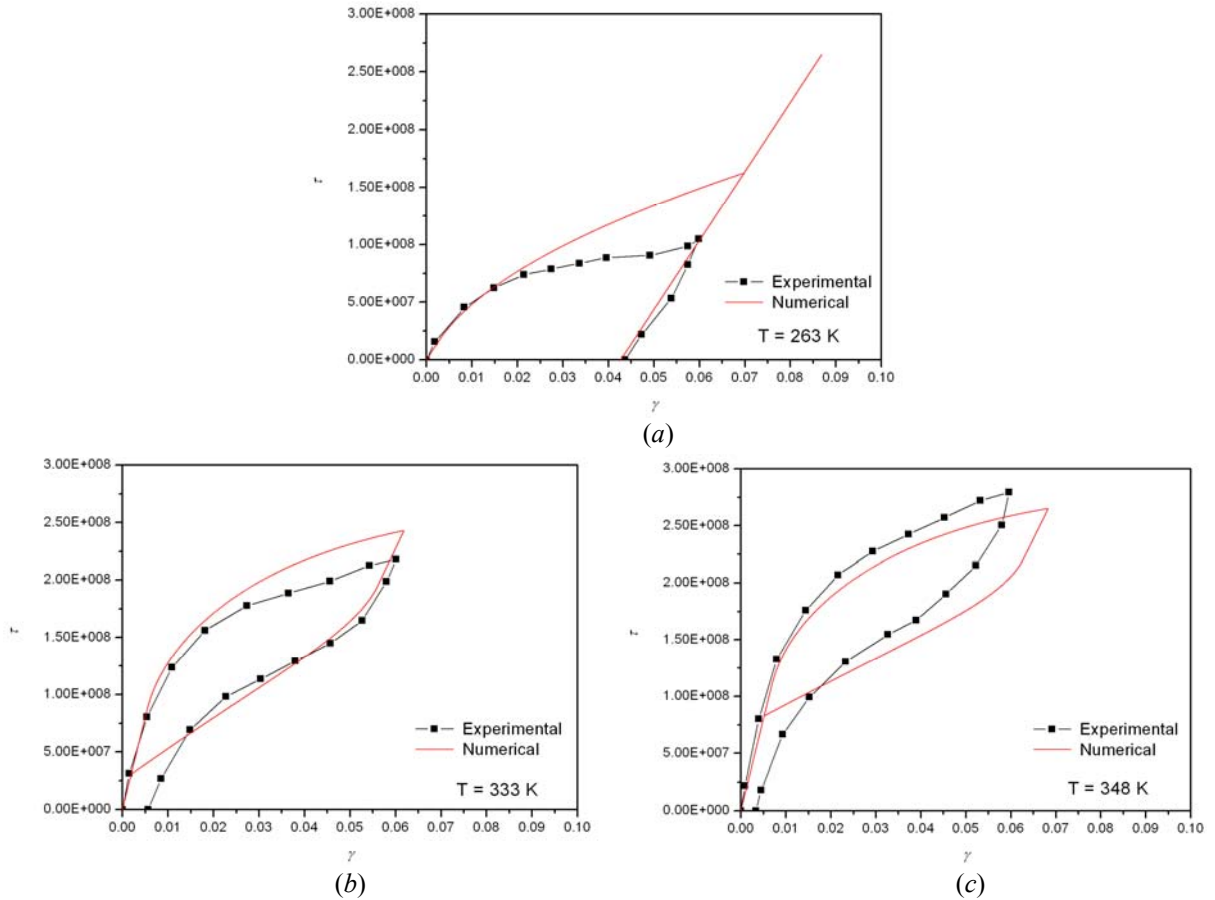


Figure 3. Stress-strain curves for shear behavior for three temperatures: (a) 263 K, (b) 333 K and (c) 348 K.

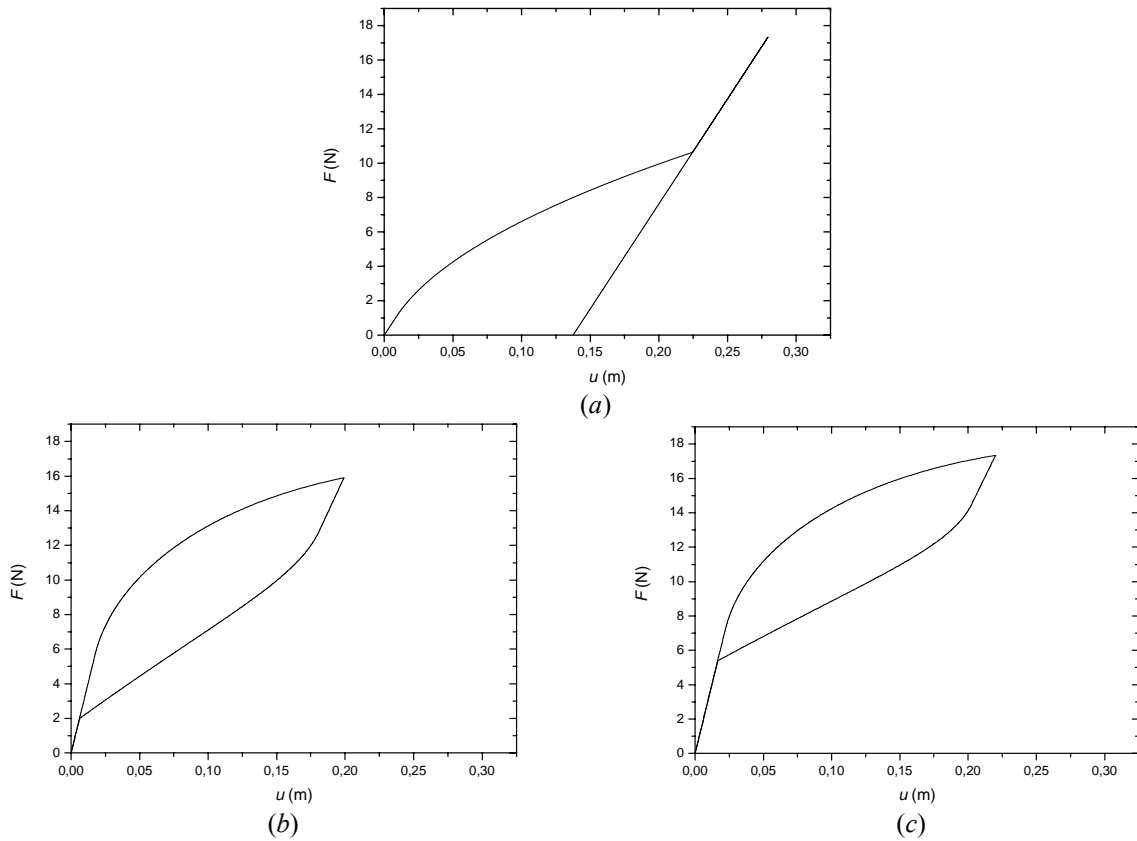


Figure 4. SMA helical spring force-displacement curves for three temperatures: (a) 263 K, (b) 333 K and (c) 348 K.

As it is well-known, SMA devices present a rate-dependence characteristic that means that the thermomechanical response depends on loading rate (Shaw & Kyriades, 1995). Some authors point that this behavior results from the thermomechanical coupling effect associated with the latent heat due phase transformation (Auricchio *et al.*, 2007; Shaw & Kyriades, 1995). The thermomechanical coupling is related to an endothermic process that occurs during the phase transformation from austenite to martensite and also an exothermic process associated with the reverse transformation. Therefore, although martensitic transformation is non-diffusive, the phase transformation critical stresses are temperature dependent and, since heat transfer process (conduction and convection) is time dependent, it affects the thermomechanical behavior of SMAs. The proposed model is rate-dependent being capable to capture this SMA characteristic without include energy equation thermomechanical terms. In order to illustrate this behavior, it is evaluated the helical spring response subjected to four different loading rates: 8 N/s, 4 N/s, 2 N/s and 1 N/s. Figure 5 presents the mechanical loadings applied to the SMA spring. This loading is applied as a ramp that reaches a magnitude of 16 N with a constant loading rate and then removed with the same loading rate.

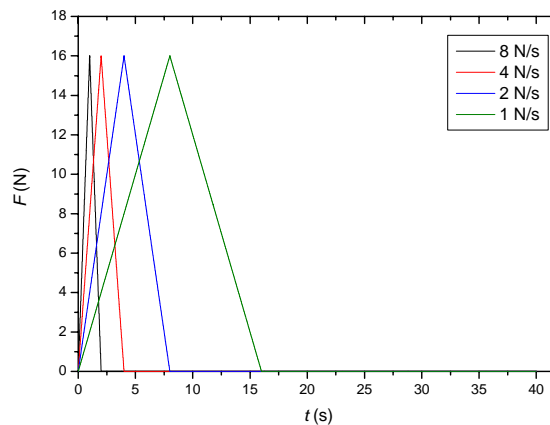


Figure 5. Thermomechanical loading considering four loading rates.

The helical spring force-displacement curves for two temperatures (263 K and 333 K) are presented in Figure 6 considering four loading rates. Shape memory and pseudoelastic effects can be observed in Figs. 6a and 6b, respectively. It should be highlighted the strong dependence on the loading rate dramatically changing the spring force-displacement curves.

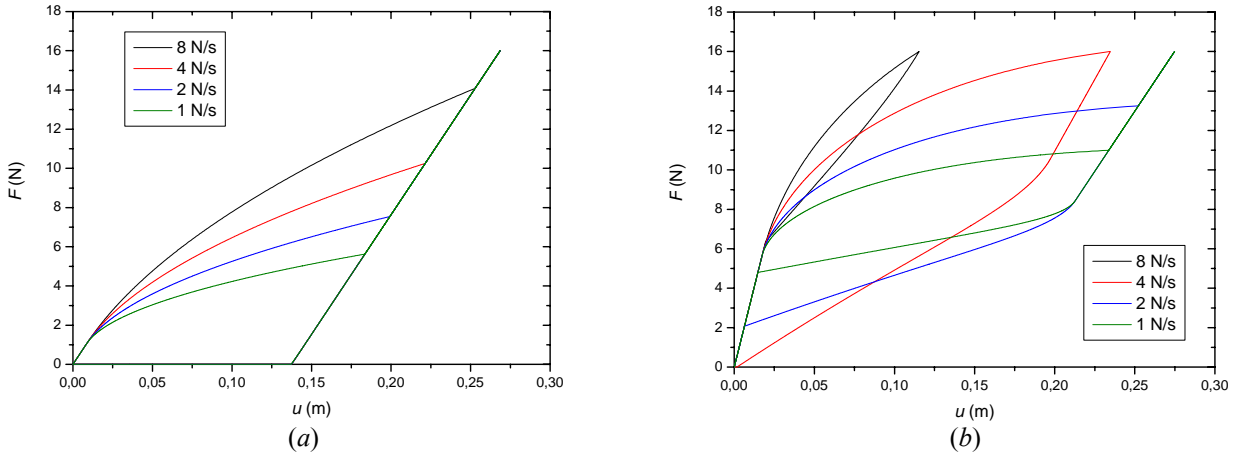


Figure 6. SMA helical spring force-displacement curves considering four different loading rates for two temperatures: (a) 263 K and (b) 333 K.

The phase transformation evolutions for the two temperatures considering the four loading rates are presented in Figures 7 and 8. Once again, it is observed a strong dependence on the loading rate. Figure 8 shows that for the largest loading rates (8 N/s and 4 N/s) are related to incomplete phase transformations.

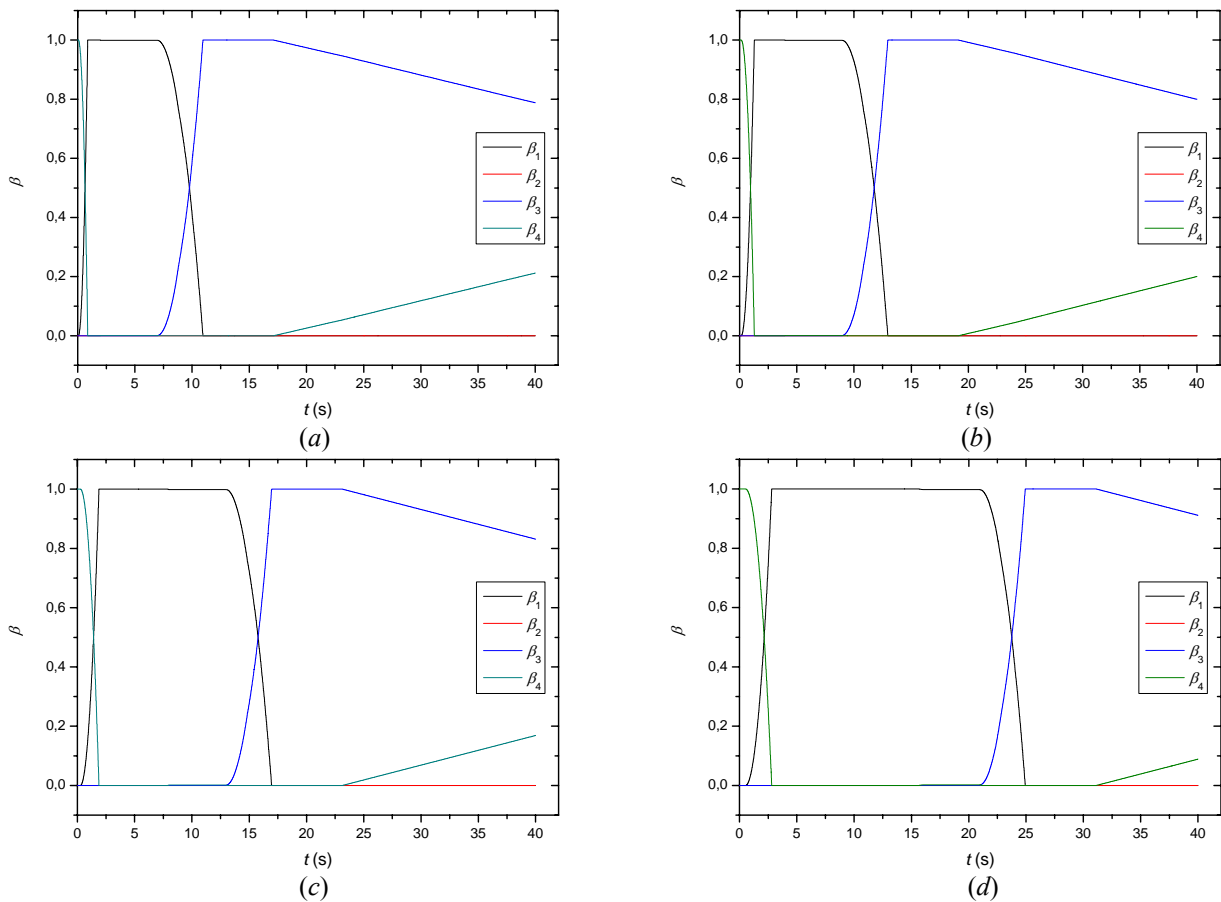


Figure 7. Phase transformation evolution for four loading rates: (a) 8 N/s, (b) 4 N/s, (c) 2 N/s and (d) 1 N/s. $T = 263$ K.

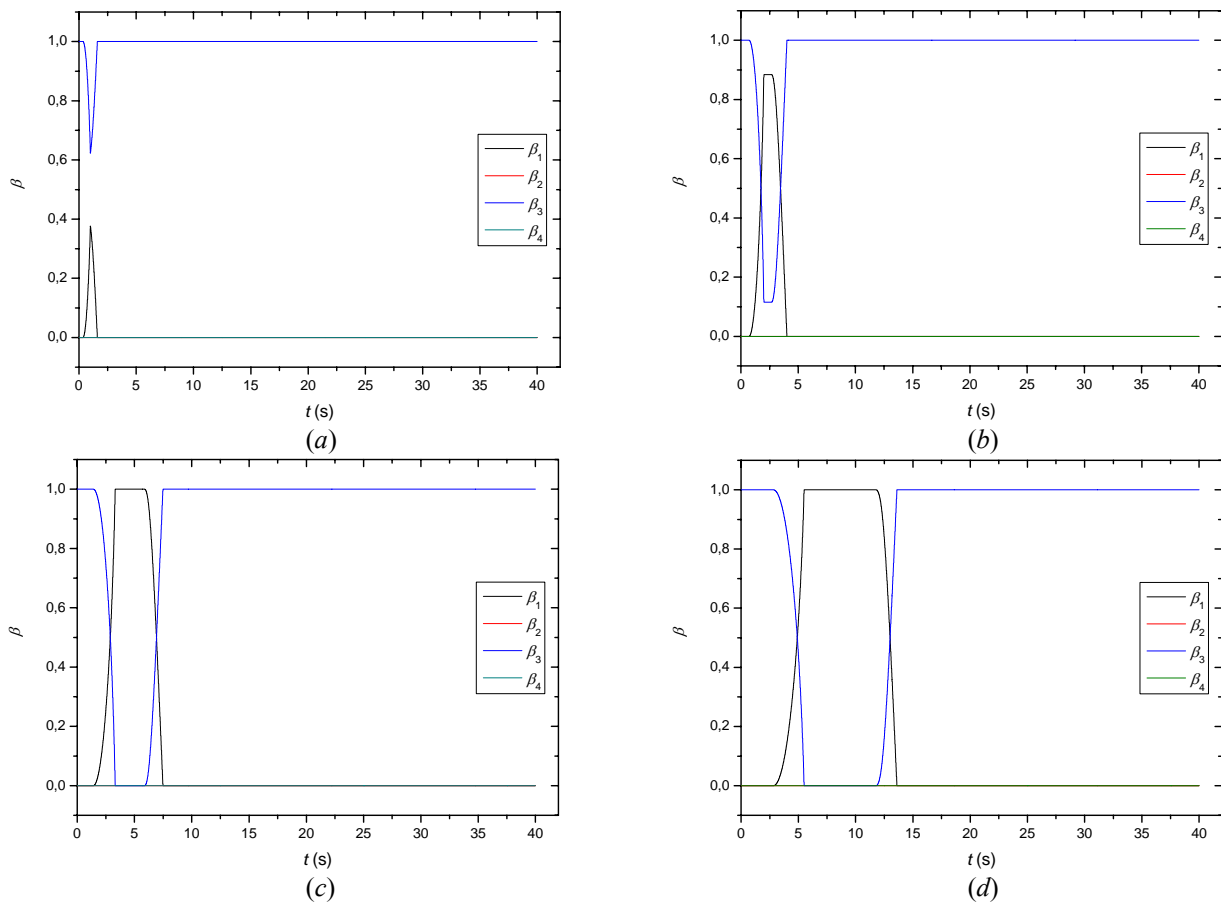


Figure 8. Phase transformation evolution for four loading rates: (a) 8 N/s, (b) 4 N/s, (c) 2 N/s and (d) 1 N/s. $T = 333\text{K}$.

SMA helical springs are usually employed as actuators in adaptive devices. In order to illustrate some characteristics of this kind of component, it is analyzed a SMA helical spring supporting a mass. A representative view of this device is shown in Fig. 9. The system is initially at thermal equilibrium and the spring being with a twined martensitic phase ($\beta_4 = 1$). At this moment, the mass is attached to the system and the spring is subjected to the action of a constant load promoted by the mass weight. This mechanical load is high enough to induce the formation of 100% of detwined martensitic phase ($\beta_1 = 1$). After this phase transformation, a heat source is applied to the spring promoting a temperature rise accomplished by a reverse phase transformation that results in a 100% austenite phase ($\beta_3 = 1$). Finally, the heat source is removed causing a new phase transformation, and the spring reaches ambient temperature with 100% of detwined martensite ($\beta_1 = 1$).

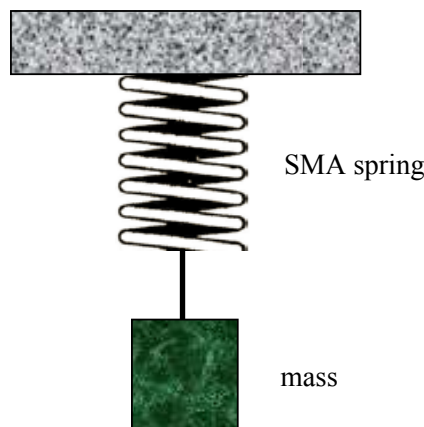


Figure 9. SMA helical spring supporting a mass.

Numerical simulations are carried out in order to describe the thermomechanical behavior of this device. The thermomechanical loading is applied in two steps. In the first one ($0 \leq t \leq 2$ s), the mechanical loading is applied to the spring as a ramp load that reaches a magnitude of 6.94 N. This load level is maintained until the end of the simulation, representing the action of the mass weight. In the second step ($2 \text{ s} \leq t \leq 24$ s), the spring temperature is prescribed through a triangular shape function that represents the application and removal of the heat source. The spring self weight is neglected assuming the initial and ambient temperatures of 285 K. A time step $\Delta t = 1 \times 10^{-3}$ s is used for simulations. Figure 10 presents the thermomechanical loading applied to the SMA spring.

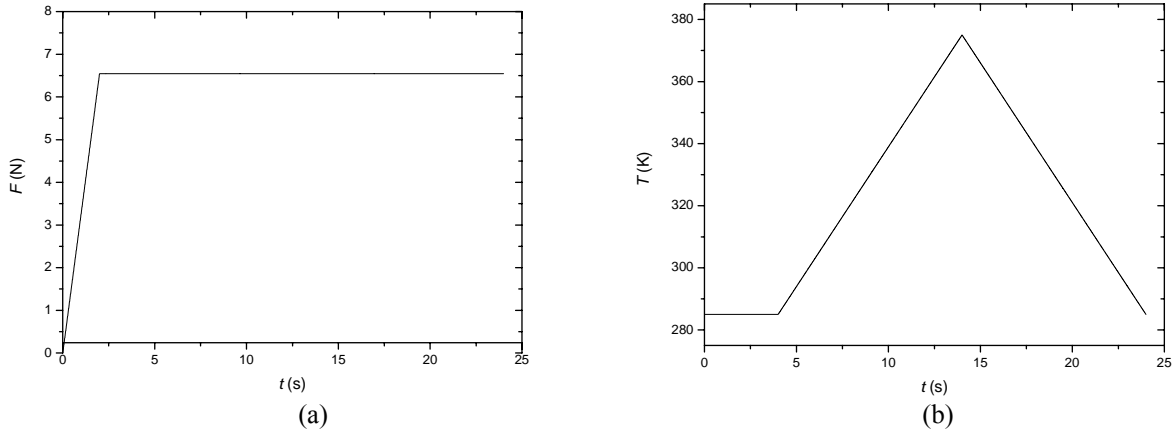


Figure 10. Thermomechanical loading. (a) Load and (b) temperature.

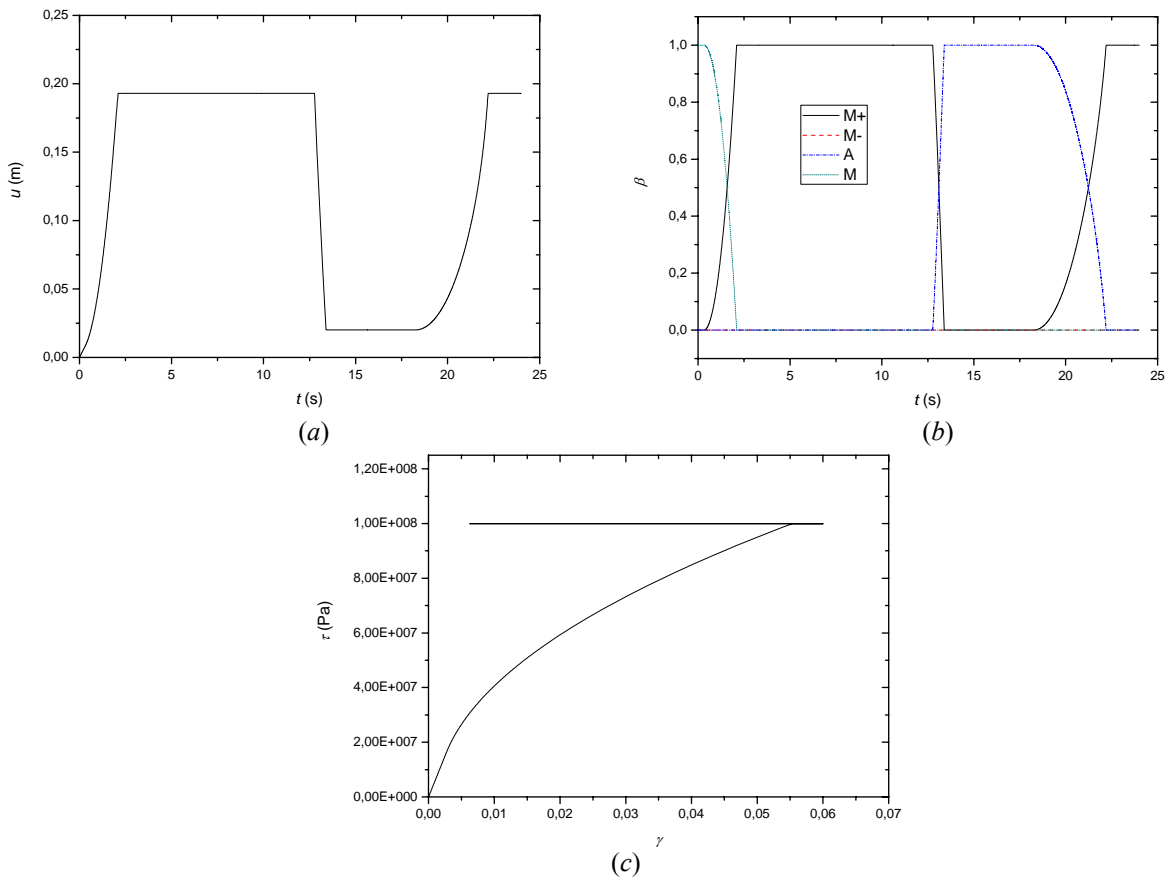


Figure 7. Displacement evolution (a), phase transformation evolution (b) and shear stress-strain curve (c).

The spring response is now in focus. Figure 11a shows the displacement evolution during the process. At first, a displacement rise is observed until a maximum value of 193 mm is reached. This displacement is developed as a consequence of the mass weight action representing approximately seven times the spring length, which indicates the SMA helical spring capability to develop very large displacements. Afterwards, it is observed a displacement reduction

due to the austenite phase formation promoted by the temperature rise. Finally, when the temperature decreases, another displacement rise is observed representing the martensitic phase formation. Figure 11b shows the volumetric fraction phase evolution during the process. Initially, it is observed the martensitic phase formation promoted by the mechanical load associated with the mass weight. After this, austenitic phase formation due to temperature rise is observed and, finally, martensitic phase formation occurs when the temperature decreases under the action of the mass weight. Figure 11c shows the spring shear stress-strain curve. The mechanical loading is observed in the nonlinear increase of stress-strain, associated with phase transformations ($A \rightarrow M^+$). The horizontal straight line, on the other hand, represents the recovery strain process that occurs when the heat source is applied promoting the formation of the austenitic phase ($M^+ \rightarrow A$) and the reverse transformation when temperature decreases ($A \rightarrow M^+$).

5. CONCLUSIONS

This contribution analyses the quasi-static response of shape memory alloys (SMA) helical springs where the restitution force is described by a one-dimensional constitutive model with internal constraints. The constitutive model includes four macroscopic phases in the formulation (three variants of martensite and an austenitic phase) and is used to describe the thermomechanical shear behavior of SMA helical springs. The basic assumption to establish the force-displacement relation from the stress-strain curve is the homogeneous phase transformation through the wire. A numerical method based on the operator split technique is developed. Numerical results show that the constitutive model is in close agreement with experimental shear tests. The SMA model rate-dependent characteristic is explored comparing responses from different loading rates. Numerical simulation considering a SMA helical spring supporting a mass shows that the proposed spring model captures the general thermomechanical behavior of SMA helical springs.

6. ACKNOWLEDGEMENTS

The authors acknowledge the support of the Brazilian Research Council - CNPq.

7. REFERENCES

- Auricchio, F., Fugazza, D., DesRoches, R., 2007, "A 1D rate-dependent viscous constitutive model for superelastic shape-memory alloys: formulation and comparison with experimental data", *Smart Materials & Structures*, v.16, n.1, S39-S50.
- Baêta-Neves, A.P., Savi, M.A. & Pacheco, P.M.C.L., 2004, "On the Fremond's constitutive model for shape memory alloys", *Mechanics Research Communications*, v.31, n.6, pp.677-688.
- Denoyer, K.K., Scott Erwin, R. and Rory Ninneman, R., 2000, "Advanced smart structures flight experiments for precision spacecraft", *Acta Astronautica*, v.47, pp.389-397.
- Fremond, M., 1987, "Matériaux à mémoire de forme", *C.R. Acad. Sc. Paris*, Tome 34, s.II, n.7, pp. 239-244.
- Fremond, M., 1996, "Shape memory alloy: A thermomechanical macroscopic theory", *CISM courses and lectures*, Springer Verlag.
- Garner, L.J., Wilson, L.N., Lagoudas, D.C., Rediniotis, O.K., 2001, "Development of a shape memory alloy actuated biomimetic vehicle", *Smart Materials and Structures*, v.9, n.5, pp.673-683.
- Jackson, C.M., Wagner, H.J. & Wasilewski, R.J., 1972, "55-Nitinol - The alloy with a memory: Its physical metallurgy, properties, and applications", NASA-SP-5110.
- Machado, L.G. & Savi, M.A., 2002, "Odontological applications of shape memory alloys", *Revista Brasileira de Odontologia*, v.59, n.5, pp.302-306 (in portuguese).
- Machado, L.G. & Savi, M.A., 2003, "Medical applications of shape memory alloys", *Brazilian Journal of Medical and Biological Research*, v.36, n.6, pp.683-691.
- Manach, P-Y. & Favier, D., 1997, "Shear and tensile thermomechanical behavior of near equiatomic NiTi alloy", *Materials Science & Engineering A*, v.222, pp.45-57.
- Ortiz, M., Pinsky, P.M. & Taylor, R.L., 1983, "Operator split methods for the numerical solution of the elastoplastic dynamic problem", *Computer Methods of Applied Mechanics and Engineering*, v.39, pp.137-157.
- Pacheco, P.M.C.L. & Savi, M.A., 1997, "A non-explosive release device for aerospace applications using shape memory alloys", *Proceedings of XIV the Brazilian Congress of Mechanical Engineering (COBEM 97 - ABCM)*, Bauru, Brazil.
- Paiva, A., Savi, M. A., Braga, A. M. B. & Pacheco, P. M. C. L., 2005, "A constitutive model for shape memory alloys considering tensile-compressive asymmetry and plasticity", *International Journal of Solids and Structures*, v.42, n.11-12, pp.3439-3457.
- Paiva, A. & Savi, M. A., 2006, "An overview of constitutive models for shape memory alloys", *Mathematical Problems in Engineering*, v.2006, Article ID56876, pp.1-30.
- Rockafellar, R. T., 1970, "Convex analysis", Princeton Press.
- Rogers, C.A., 1995, "Intelligent materials", *Scientific American*, September, pp.122-127.

- Savi, M. A. and Braga, A. M. B., 1993a, "Chaotic vibrations of an oscillator with shape memory", *Journal of the Brazilian Society of Mechanical Sciences and Engineering*, v.XV, n.1, pp.1-20.
- Savi, M. A. & Braga, A. M. B., 1993b, "Chaotic response of a shape memory oscillator with internal constraints", *Proceedings of XII the Brazilian Congress of Mechanical Engineering (COBEM 93 - ABCM)*, Brasilia, Brazil, pp.33-36.
- Savi, M. A., Paiva, A., Baêta-Neves, A. P. & Pacheco, P. M. C. L., 2002, "Phenomenological modeling and numerical simulation of shape memory alloys: A thermo-plastic-phase transformation coupled model", *Journal of Intelligent Material Systems and Structures*, v.13, n.5, pp.261-273.
- Savi, M.A. & Paiva, A., 2005, "Describing internal subloops due to incomplete phase transformations in shape memory alloys", *Archive of Applied Mechanics*, v.74, n.9, pp.637-647.
- Shaw, J. A. & Kyriades, S., 1995, "Thermomechanical Aspects of Ni-Ti", *Journal of the Mechanics and Physics of Solids*, v. 43, n. 8, pp. 1243-1281.
- Tobushi, H. & Tanaka, K., 1991, "Deformation of a shape memory alloy helical spring - (Analysis based on stress-strain-temperature relation)", *JSME International Journal Series I - Solid Mechanics Strength of Materials*, v.34, n.1, pp.83-89.
- Toi, Y., Lee, J-B. & Taya, M., 2004, "Finite element analysis of superelastic, large deformation behavior of shape memory alloy helical springs", *Computer & Structures*, v.82, pp.1685-1693.
- van Humbeeck, J., 1999, "Non-medical applications of shape memory alloys", *Materials Science and Engineering A*, v.273-275, pp.134-148.
- Webb, G., Wilson, L., Lagoudas, D.C. & Rediniotis, O., 2000, "Adaptive Control of Shape Memory Alloy Actuators for Underwater Biomimetic Applications", *AIAA Journal*, v.38, n.2, pp. 325-334.

8. RESPONSIBILITY NOTICE

The authors are the only responsible for the printed material included in this paper.